Fluids and Barriers of the CNS

RESEARCH

Open Access

High affinity of β-amyloid proteins to cerebral capillaries: implications in chronic lead exposure-induced neurotoxicity in rats

Luke L. Liu[1], Xiaoli Shen[1,2], Huiying Gu[3], Gang Zhao[1,4], Yansheng Du[3] and Wei Zheng[1*]

Abstract

Lead (Pb) is a known environmental risk factor in the etiology of Alzheimer's disease (AD). The existing reports suggest that Pb exposure increases beta-amyloid (Aβ) levels in brain tissues and cerebrospinal fluid (CSF) and facilitates the formation of amyloid plaques, which is a pathological hallmark for AD. Pb exposure has long been associated with cerebral vasculature injury. Yet it remained unclear if Pb exposure caused excessive Ab buildup in cerebral vasculature, which may damage the blood–brain barrier and cause abnormal Ab accumulation. This study was designed to investigate the impact of chronic Pb exposure on Aβ accumulation in cerebral capillary and the expression of low-density lipoprotein receptor protein-1 (LRP1), a critical Aβ transporter, in brain capillary and parenchyma. Sprague–Dawley rats received daily oral gavage at doses of 0, 14 (low-dose), and 27 (high-dose) mg Pb/kg as Pb acetate, 5 d/wk, for 4 or 8 wks. At the end of Pb exposure, a solution containing $A\beta_{40}$ was infused into the brain via the cannulated internal carotid artery. Data by ELISA showed a strikingly high affinity of Ab to cerebral vasculature, which was approximately 7–14 times higher than that to the parenchymal fractions collected from control brains. Pb exposure further aggravated the Aβ accumulation in cerebral vasculature in a dose-dependent manner. Western blot analyses revealed that Pb exposure decreased LRP1 expression in cortical capillaries and hippocampal parenchyma. Immunohistochemistry (IHC) studies further revealed a disrupted distribution of LRP1 alongside hippocampal vasculature accompanied with a decreased expression in hippocampal neurons by Pb exposure. Taken together, the current study demonstrated that the cerebral vasculature naturally possessed a high affinity to Aβ present in circulating blood. Pb exposure significantly increased Aβ accumulation in cerebral vasculature; such an increased Aβ accumulation was due partly to the diminished expression of LRP1 in response to Pb in tested brain regions. Perceivably, Pb-facilitated Ab aggravation in cerebral vasculature may contribute to Pb-associated amyloid alterations.

Highlights

1. Affinity of $A\beta_{40}$ to cerebral vasculature was exceptionally high.
2. Pb exposure exacerbated $A\beta_{40}$ accumulation in cerebral vasculature.
3. LRP1 expression was disrupted by Pb in brain parenchyma and vasculature.

*Correspondence:
Wei Zheng
wzheng@purdue.edu
Full list of author information is available at the end of the article

Keywords Lead (Pb), Amyloid beta (Aβ), Cerebral vasculature, Low density lipoprotein receptor-related protein 1 (LRP1)

Introduction

Aggregation of beta-amyloid (Ab) peptides in the brain extracellular space to form the insoluble plaques is the hallmark of Alzheimer's disease (AD). Excess accumulation of Ab in the cortex and hippocampus initiates the detrimental cellular cascades leading to the progressive degeneration of neurons and the ensuing cognitive deficits [33]. In AD brains, Ab is found in the cerebrospinal fluid (CSF) circulating in brain ventricles, in the interstitial fluid (ISF) bathing neurons and glial cells and in cerebral vasculature [42, 49, 51, 61]. Elevated Ab levels in brain extracellular space may result from an increased production of Ab peptides due primarily to genetic predisposition and/or a decreased clearance of Ab from the brain.

Sporadic cases account for over 90% of AD, suggesting a substantial contribution of environmental factors such as exposure to neurotoxic metal lead (Pb). Indeed, human studies have shown strong associations between lifetime Pb exposure and progressive cognitive declines and brain structural damages [19, 32, 48]. The presence of a high level of Pb in diffuse neurofibrillary tangles, a form of presenile dementia, has been shown in 10 AD cases compared with 9 controls [24]. The formation of senile plaques is evident in a patient exposed to Pb at age of 2.3 years old with a confirmed Pb encephalopathy and died at 42 [36]. Mechanistic studies using animal models also suggest causal associations of early-life Pb exposure with epigenetic alterations, amyloid plaque formation, and late-onset AD [67]. Research by this group has demonstrated that chronic Pb exposure accelerates the Aβ plaque formation and increases cognitive deficits in an AD transgenic mouse model (Tg-SWDI) [20, 22]. Interestingly, the Tg-SWDI mice possess a relatively high ratio of $A\beta_{40}$ to $A\beta_{42}$ and exhibit substantial cerebral amyloid angiopathy (CAA); such pathologies were further aggravated by chronic Pb exposure, leading to an even higher level of brain $A\beta_{40}$ that is typically seen in CAA [20, 22].

Literature reports also provide evidence to support a linkage between Pb exposure and cerebral vasculature injury. For example, cerebral vasculature shows a higher propensity to accumulate Pb than do other brain cell types [56, 58, 74]. Pb exposure causes the damage to the cerebral vasculature that constitutes the blood–brain barrier (BBB) [25, 63, 74]. In addition, Pb exposure targes both heart and vascular smooth muscle and causes hypertension [41, 43, 59, 60]. Noticeably, "seeding" of exogenous Aβ from the peripheral circulation likely triggers an extensive Ab aggregation in the brain [2, 28]. Indeed, amyloid species exist in the blood circulation, with the concentrations increased in AD patients [26]. Considering the combined effects of Pb exposure, brain microvascular injury, and the ensuing amyloid accumulation, it is reasonable to postulate that Pb exposure may cause abnormal Aβ accumulation in cerebral vasculature, which may contribute to Pb-induced AD pathogenesis. However, the question as to whether Pb exposure increased $A\beta_{40}$ buildup in cerebral vasculature has never been investigated.

The homeostasis of Aβ in brain extracellular fluids is maintained by a number of Aβ binding and transporting proteins. In general, the receptor for advanced glycation endproducts (RAGE) is believed to be a primary transporter at the BBB that transports Aβ from the blood to brain parenchyma (i.e., influx) [11] and the low-density lipoprotein receptor-related protein 1 (LRP1) serves as the main transporter of Aβ from brain to the blood (i.e., efflux) [13, 39]. Previous studies from this lab have established that Pb exposure increases Aβ levels in the choroid plexus, a barrier between the blood and CSF; this increase is concurrent with a decreased expression of LRP1 [22] and the abnormal intracellular trafficking of LRP1 in choroidal epithelia [3, 52]. Nonetheless, it remained unknown if Pb overload in brain capillaries would alter LRP1 expression and therefore affect Aβ efflux in the BBB.

The main purposes of the present study were to investigate whether and how in vitro and in vivo Pb exposure affected the accumulation of Aβ in the cerebral vasculature. We used in situ brain infusion technique to deliver $A\beta_{40}$ molecules directly into the brain via the internal carotid artery, followed by a capillary depletion procedure to separate the cerebral vasculature from parenchyma, allowing to quantify Aβ concentrations in cerebral vasculature and brain parenchymal fractions from various brain regions. We further analyzed the expression of LRP1 in regional vascular and parenchymal fractions with a particular focus on hippocampus. The results may shed light on the mechanism by which Pb exposure causes AD pathology.

Material and methods

Materials

Chemical reagents and assay kits were purchased from the following sources: lead acetate trihydrate ($PbAc_2{\cdot}3H_2O$), sodium pyruvate, calcium chloride

($CaCl_2$), Dextran-70, HEPES, 2-mercaptoethanol, phenylmethylsulfonyl fluoride (PMSF), poly-acrylamide and tetramethyl-ethylenediamine (TEMED) from Sigma Chemicals (St Louis, MO); ultrapure nitric acid from VWR international (Chicago, IL); protease inhibitor cocktail from Calbiochem (San Diego, CA); Tris-base, glycine, sodium dodecyl sulfate (SDS), 2X Laemmli sample buffer, Triton X-100, and Clarity Western ECL substrate from Bio-Rad (Hercules, CA); human $A\beta_{40}$ recombinant peptides, human $A\beta_{40}$ ELISA kit from Invitrogen, goat anti-rabbit secondary antibody conjugated with Alexa Fluor 488, goat anti-rat secondary antibody conjugated with Cyanine5, goat anti-rabbit secondary antibody conjugated with horseradish peroxidase (HRP), and goat anti-mouse secondary antibody conjugated with HRP from Invitrogen (Waltham, MA); and Dextran (75,000) from Spectrum Chemicals (Gardena, CA). Sources of primary antibodies and dilution factors are listed in Table 1. All reagents were of analytical grade, HPLC grade, or the best available pharmaceutical grade.

Animals

Mice were initially used for concept-proving preliminary in vitro studies as described in "Preparation of cerebral capillary fraction and in vitro Aβ40 affinity study" section. Most of the experiments in this report were performed using rats for technical feasibility of in situ brain perfusion and large yields of capillary fraction. C57BL/6 mice (3 months old) and Sprague Dawley rats (10 weeks old) were purchased from Harlan Sprague Dawley Inc. (Indianapolis, IN). Literature data suggest that the animal strains used in this study with a wild type background develop no Aβ pathologies at the time of our experiments [4, 38], indicating a minimal level of endogenous Aβ. Upon arrival, animals were housed in a temperature-controlled room under a 12-h light/12-h dark cycle and allowed to acclimate for one week prior to experimentation. Animals had free access to deionized water and pellet rat chow (Teklad Dlobal 18% Protein Rodent Diet, 2018s; Envigo) ad libitum. This study was conducted in compliance with standard animal use and practice and was approved by Purdue Animal Care and Use Committee (PUCAC No. 1112000526).

Table 1 Primary antibodies and dilutions used for Western Blot and IHC studies

Target	Dilution (application)	Host species	Source and identifier
LRP1	1:1000 (WB); 1:200 (IHC)	Rabbit	Abcam ab92544
Beta-actin	1:2000 (WB)	Mouse	Sigma-Aldrich A5316
CD31	1:500 (IHC)	Rat	Invitrogen MA1-40074

Preparation of cerebral capillary fraction and in vitro $A\beta_{40}$ affinity study

Under deep anesthesia, animals were transcardially perfused with ice-cold PBS and the brains were carefully extracted. Cerebral vasculature was separated using a well-established "capillary depletion" method in this lab [7, 12, 14] (as illustrated in Fig. 1A). Briefly, ice-chilled brain samples were weighted and transferred to a 1-ml glass tissue grinder (Wheaton, Millville, NJ, followed by addition of 3 volumes of ice-cold homogenization buffer [HB solution (g/mL); brain weight/HB volume, which consisted of the following chemicals with their final concentrations: HEPES 10 mmol/L, NaCl 141 mmol/L, KCl 4 mmol/L, $MgSO_4$ 1.0 mmol/L, NaH_2PO_4 1.0 mmol/L, $CaCl_2$ 2.5 mmol/L, and glucose 10 mmol/L (pH 7.4)]. The entire brain from mice or separate brain regional tissues from rats were homogenized by eight strokes, followed by addition of another 4 volumes of 30% Dextran-70 solution in a final ratio of 1:3:4 (brain: HB: dextran-70). The mixture was then homogenized for three additional strokes. After centrifugation at 5400×*g* for 15 min at 4 °C, the supernatant (capillary-depleted parenchyma) and the pellet (capillary-enriched fraction) were separated carefully. The presence of networks of brain vessels in the pellet and a vasculature-depleted supernatant were confirmed by light microscopy. Notably, although this method represents an effective approach for vasculature-parenchyma separation, isolated vasculature can still somewhat contain, besides endothelial cells, other cell types such as vascular smooth muscle cells and pericytes [40].

To prove the concept of Pb altering $A\beta_{40}$ affinity to cerebral capillaries, an in vitro study to incubate cerebral capillary with $A\beta_{40}$ was conducted. Freshly separated cerebral capillaries were incubated in the control HBSS buffer (supplemented with 0.5% BSA) without Pb or in the HBSS containing Pb concentration at 10 μM for 24 h, after which $A\beta_{40}$ was added to the culture medium at a final concentration of 1 μM. The incubation continued for 30 min at room temperature with gentle rotation. Upon completion of incubation with $A\beta_{40}$, the capillary samples were washed with HBSS three times to remove the unbound $A\beta_{40}$. Capillaries were then lysed in 5 M guanidine-HCl for 1 h at room temperature and quantified for $A\beta_{40}$ concentrations using enzyme-linked immunosorbent assay (ELISA) (detailed in "Quantification of Aβ40 in both parenchyma and capillary by ELISA" section).

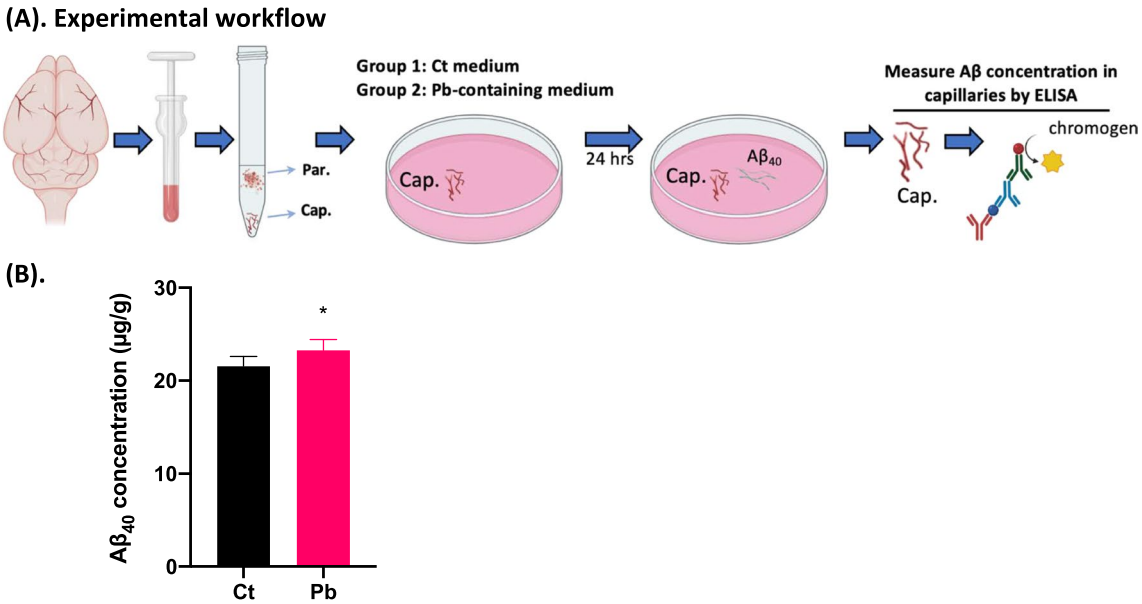

Fig. 1 Increased Aβ binding to cerebral capillaries following in vitro Pb exposure. **A** Graphical illustration of the experimental workflow to assess $A\beta_{40}$ affinity as affected by Pb exposure using freshly separated cerebral capillaries in vitro. **B** ELISA quantification of $A\beta_{40}$ concentration in control or Pb-pretreated cerebral capillaries. Data represent mean ± SD, n = 6; *$p < 0.05$. *Par.* parenchyma fraction, *Cap.* capillary fraction

In vivo Pb exposure and in situ brain perfusion

$PbAc_2{\cdot}3H_2O$ was dissolved in sterile saline for oral gavage. Rats were exposed to Pb by oral gavage at doses of 14 and 27 mg Pb/kg, as low- (LD-Pb) and high-dose (HD-Pb) group, respectively (the control received the same volume of saline), once daily, 5 days/week, for 4 or 8 consecutive weeks. This Pb exposure dosing regimen was used based on our prior studies, in which the blood Pb levels in Pb-exposed animals were similar to those observed in occupational workers [21, 52].

Following Pb exposure for 4 or 8 weeks, in situ brain perfusion was conducted to investigate how Pb exposure affected the $A\beta_{40}$ affinity to cerebral capillaries and brain parenchyma. This technique has been routinely used by this laboratory for studies such as trace element metal copper (Cu) and Aβ peptide uptake by BBB and blood-CSF barrier (BCB) [14, 31, 52]. Briefly, 24 h after last gavage, rats were anesthetized by ketamine/xylazine (75:10 mg/kg, ip) and placed on a heating pad in a supine position. The right common carotid artery was isolated, and a small cut was made. A polyethylene catheter (PE-10) tubing (prefilled with Ringer's solution and connected with a peristaltic pump through a 3-way stopcock) was then carefully inserted into the artery toward the brain. The inserted tubing was then fixed by a surgical suture, followed by a ligation of the external carotid artery to ensure the flow of the perfusate entering exclusively to the internal carotid artery, which supplies blood for the brain.

The brain was perfused with Ringer's solution (warmed to 37 °C and continuously gassed with 95% O_2/5% CO_2) by a Mini-Pump (VWR, Radnor, PA) at 9 mL/min. The second syringe pump (pre-connected with the 3-way stopcock) was subsequently turned on to infuse Ringer's solution containing $A\beta_{40}$ at 25 μg/mL with a flowrate of 1 mL/min. The total flow rate of perfusion by two pumps was 10 mL/min with the infusate ($A\beta_{40}$) concentration at 2.5 μg/mL. Considering the high flowrate (10 mL/min) and Pb's cytosol accumulation (sequestration by intracellular glutathione or metallothionein), it is anticipated that $A\beta_{40}$ in the perfusate has little direct contact with Pb; hence, any alteration in $A\beta_{40}$ affinity to capillaries is considered due primarily to the interaction between $A\beta_{40}$ molecules and endothelial cells through surface binding and intracellular uptake. The in-situ brain perfusion with $A\beta_{40}$ lasted 2 min. To prevent blood recirculation, the left ventricle of the heart was cut upon the start of the perfusion. After 2-min $A\beta_{40}$ perfusion, the pump with $A\beta_{40}$ solution was shut off and the pump with only Ringer's solution was left on for 1 min to remove $A\beta_{40}$ adsorbed to the luminal surface.

At the end of brain perfusion, the brains were extracted from the skull; hippocampus, frontal cortex and the rest of brain tissues were dissected for capillary-parenchyma separation as described in "Preparation of cerebral capillary fraction and in vitro Aβ40 affinity study" section. Concentrations of $A\beta_{40}$

in the collected vascular and parenchyma fractions were measured by ELISA following manufacturer's instructions.

Quantification of $A\beta_{40}$ in both parenchyma and capillary by ELISA

Total proteins of brain capillary and parenchyma were extracted with a buffer containing 50 mmol/L Tris–HCl, 150 mmol/L NaCl, 1% Nonidet P-40, 0.5% sodium deoxycholate, 1 mmol/L EDTA, and a protease inhibitor cocktail. The protein concentrations were determined using the Bradford assay. Levels of $A\beta_{40}$ were assayed by sandwich ELISA as previously described per manufacturer's instructions [22, 52]. Briefly, the protein extracts of capillary and parenchymal fractions of hippocampus, cortex and the rest of brain were incubated in 96-well ELISA plates that had been coated with $A\beta_{40}$-capturing antibodies. Subsequently, $A\beta_{40}$-detector antibodies were added and incubated for 3 h at room temperature. Following sufficient washes to remove the unbound antibodies, IgG HRP solution was added to bind the detector antibodies; the wells were covered and incubated for 30 min at room temperature. Through thorough washes, chromogen solutions were added to each well and continued to incubate at room temperature for 30 min under dark. After addition of stop solutions, the plates were read for absorbance at 450 nm. The concentration of $A\beta_{40}$ in the tissues was reported as ng/g of total protein.

Western blot (WB)

WB assay was performed as previously described [31]. Briefly, the extracted protein samples from brain regional capillaries and parenchyma were diluted with sample buffer to the final protein concentrations of appropriately 2 mg/mL. Protein samples were mixed with 2× Laemmli sample buffer and boiled for 5 min. Samples (10 µL containing 10 µg protein) were then loaded on the 8 + 15% dual-layer tris–glycine SDS–polyacrylamide gels, electrophoresed and transferred to PVDF membranes. The membranes were blocked with 5% dry milk (fat free) in Tris-buffered saline with 0.1% Tween 20 (TBST) and incubated overnight at 4 °C with the primary antibodies. Following sufficient washes by TBST, PVDF membranes were further incubated with HRP-conjugated secondary antibodies at room temperature for 1 h. The colorimetric signals on the membranes were developed using ECL Western Blotting substrate by Molecular Imager and captured by ChemiDoc XRS + Software (Bio-Rad, Hercules, CA). Beta-actin was used as an internal control. The band intensities were quantified using ImageJ and were reported as relative expression levels to beta-actin.

Immunohistochemistry (IHC)

At the end of in vivo Pb exposure, rat brain samples were prepared for IHC characterization of LRP1 expression as previously described [31]. Briefly, 4% paraformaldehyde (PFA)-perfused brain samples were further fixed in this fixative solution under 4 °C overnight. Following dehydration in 30% sucrose solution, brains samples were treated into 40-µm brain slices by a microtome, and then preserved in cryopreservation medium (30% sucrose, 1% polyvinylpyrrolidone, 30% ethylene glycol in 0.1 M phosphate buffer) under −20 °C. Upon IHC staining, brain slices with regions of interest were collected and washed with PBS 3 times. The subsequent blocking was performed by incubating brain slices in PBST containing 5% normal goat serum (NGS) and 0.3% TritonX-100 for 1 h at room temperature. Blocked slices were then incubated with primary antibodies targeting LRP1 and CD31 overnight at 4 °C. Following 3× PBST washes, brain slices were further incubated with fluorophore-conjugated secondary antibodies (1:500) for 1 h at room temperature prevented from light. Following 3× PBST washes, stained slices were mounted onto microscope slides with mounting medium containing DAPI. Negative control staining was performed using the same procedures except for the primary antibody incubation step: following blocking with NGS, slices directly incubated with secondary antibodies and DAPI (image provided in Additional file 1: Fig. S1). The IHC images were captured by Nikon A1Rsi Confocal system. To quantitatively assess expression of LRP1 in response to Pb exposure, fluorescent intensity of LRP1 in anatomically matched regions was quantified using ImageJ in known neuron-rich regions for neuronal and in CD31(+) cells for endothelial assessment. LRP1 fluorescent intensity was normalized against the control group measurements for statistical analysis.

Determination of Pb concentrations by atomic absorption spectrophotometry (AAS)

Pb concentrations in blood or tissues were quantified by AAS as described in our previous publications [52, 75]. Samples (200 mg of wet weight) were digested in a MARSX press microwave-accelerated reaction system with 0.20 mL ultrapure concentrated nitric acid at 200 °C for 4 h. Blood samples (200 mL) were digested with nitric acid in the oven at 55 °C overnight. An Agilent Technologies 200 Series SpectrAA with a GTA 120 graphite tube atomizer was used to quantify Pb concentrations. The standard curves were prepared daily at concentrations of 0, 4, 8, 12, 16, and 20 µg/L with correlation coefficient of $r^2 = 0.9869$. The detection limit was 1.35 ng Pb/mL of assay solution. The intra-day and inter-day precisions of the method were 1.5% and 2.9%, respectively.

Statistical analysis

All data are presented as mean ± standard deviation (SD). Statistical analyses of the differences between control and Pb-exposed group(s) were carried out by Student's t-test or one-way ANOVA with post hoc comparisons by the Dunnett's test. All the statistical analyses were conducted using GraphPad Prism (San Diego, CA). The differences between two means were considered significant if p values were equal or less than 0.05.

Results

In vitro Pb exposure increased $A\beta_{40}$ binding to the cerebral capillaries

To test the concept that Pb increased the binding of amyloid species to cerebral vasculature, we conducted a preliminary study by preparing cerebral capillaries freshly isolated from normal mouse brains and pre-incubating the capillary preparation with Pb for 24 h, followed by incubation with $A\beta_{40}$ in the medium (Fig. 1A). Data by ELISA quantification revealed that Pb treatment significantly increased the $A\beta_{40}$ concentrations in the cerebral capillaries by 7.88%, as compared to controls ($p < 0.05$) (Fig. 1B). This in vitro finding suggested that Pb exposure appeared likely to facilitate the Aβ accumulation in cerebral vasculature. This observation led to the following in vivo validation and characterization.

In vivo chronic Pb exposure induced excessive $A\beta_{40}$ affinity by cerebral capillaries

In situ brain perfusion is a unique technique to study substance's uptake en route from the cerebral vasculature to parenchyma, for its direct delivery of testing molecules into the cerebral artery with a subsequent quantitation of the partition of the testing molecule between blood vessels and parenchyma. In the current study, rats were chosen for surgical convenience and the large yield of capillary fraction. Figure 2A depicts the workflow of in vivo Pb exposure dose regimen, in situ brain perfusion, capillary/parenchyma separation, and assays used. Data by AAS demonstrated that the blood lead levels (BLLs) were 15–25 mg/dL and 10-23 mg/dL, in rats following 4 and 8 weeks of Pb oral gavage exposure, respectively (Fig. 2B, D). Correspondingly, Pb concentrations in hippocampus, frontal cortex and other regions were significantly increased in Pb-exposed animals (Fig. 2C, E).

On these Pb-exposed and control animals, we performed a 2-min in situ perfusion of $A\beta_{40}$; ELISA was then used to quantify $A\beta_{40}$ concentration in cerebral capillary and parenchyma fractions. Our data showed that under normal physiological condition, the average $A\beta_{40}$ in normal hippocampal capillary from control rats without Pb exposure was 9.9 times higher than that in normal hippocampal parenchyma ($p < 0.01$). Similarly, the average $A\beta_{40}$ in normal cortex capillary is 11.7 times higher than that in cortex parenchyma ($p < 0.05$) (Fig. 3A). Thus, it became apparent that the degree to which $A\beta_{40}$ molecules bound to the cerebral capillaries, regardless of brain regions, far exceeded their binding to parenchyma (Fig. 3A, B), suggesting a naturally high binding affinity of $A\beta_{40}$ to cerebral vasculature.

Chronic Pb exposure clearly increased $A\beta_{40}$ accumulation in capillary and parenchymal fractions. Following 4-week Pb exposure, the $A\beta_{40}$ levels in hippocampal capillaries were significantly increased by 65.3% ($p < 0.05$) and 122.9% ($p < 0.01$) in the low and high Pb exposure group, respectively, as compared to controls (Fig. 3A). The 8-week Pb exposure induced similar dose-dependent $A\beta_{40}$ accumulation in hippocampal capillaries (Fig. 3B). In addition, Pb exacerbated $A\beta_{40}$ accumulation in cerebral capillaries isolated from the frontal cortex, but to a degree less than that in hippocampus. For example, concentrations of $A\beta_{40}$ in the frontal capillary, following 4 weeks of high-dose Pb exposure, was elevated by 17.0% ($p < 0.05$), but not in the low exposure group, as compared with controls. After 8 weeks of exposure, the $A\beta_{40}$ levels in frontal cortex capillaries were increased by 38.8% and 48.2% in the low and high Pb exposed animals ($p < 0.05$), respectively, versus controls.

In contrast, the concentrations of $A\beta_{40}$ detected in brain parenchyma were much lower than those in cerebral capillaries (Fig. 3A, B). Among tested brain regions, hippocampal parenchyma was most susceptible to Pb-elevated $A\beta_{40}$ deposition. A 4-week Pb exposure increased $A\beta_{40}$ detected in this fraction by 18–20% in both Pb-treated groups in comparison to controls ($p < 0.05$). Pb exposure for 8 weeks at the high level increased even more $A\beta_{40}$ deposition in hippocampal parenchyma by 36.5% ($p < 0.05$), while the low-level exposure for 8 weeks did not alter $A\beta_{40}$ levels. The parenchymal fractions collected from the frontal cortex and the rest brain regions showed the similar trend in accumulating $A\beta_{40}$, following in vivo Pb exposure at low- and high-doses for 4 or 8 weeks (Fig. 3A, B).

Overall, the observations from our in situ perfusion study suggested that cerebral vasculature possessed an intrinsic high affinity to $A\beta_{40}$ present in blood circulation; chronic Pb exposure seems likely to render the cerebral vasculature more venerable to $A\beta_{40}$ accumulation.

Pb exposure decreased LRP1 expression in specific fractions of hippocampus, frontal cortex, and other regions

To understand the mechanism by which Pb increased $A\beta_{40}$ deposition in cerebral vasculature and brain parenchyma, we performed Western blot to determine LRP1 expression in collected brain factions with or without Pb exposure, since LRP1 is known to transport $A\beta_{40}$

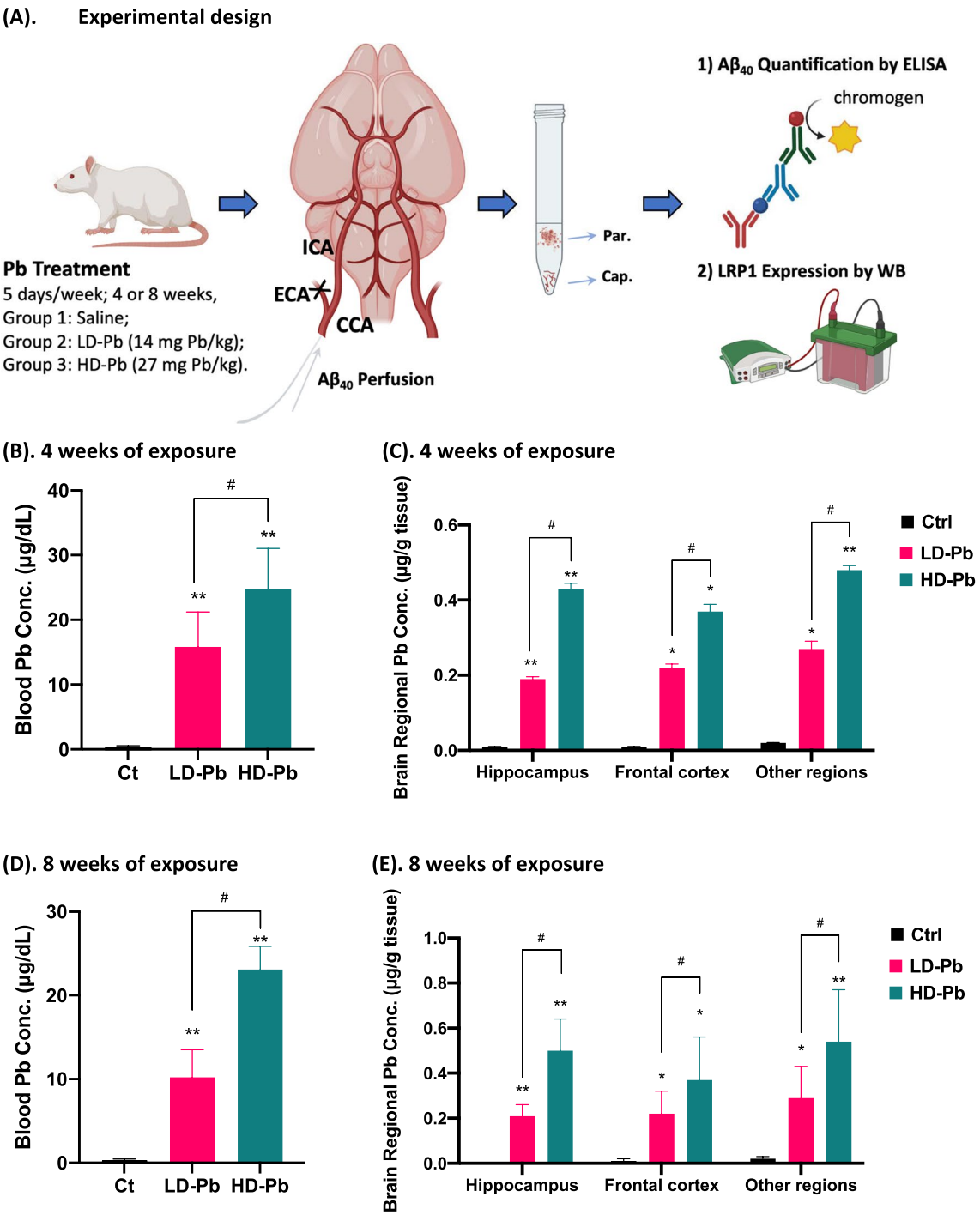

Fig. 2 Experimental design of chronic in vivo Pb exposure and Pb levels in rat blood and selected brain tissues. **A** Graphical illustration of the experimental design to study the $A\beta_{40}$ affinity to cerebral capillaries (cap.) and parenchyma (par.) via in situ brain perfusion technique and the effects of chronic Pb exposure. Capillary and parenchyma fractions of hippocampus, frontal cortex, and other brain regions were separated using a capillary depletion procedure for ELISA quantification of $A\beta_{40}$ concentration; Western blot (WB) was performed to assess the LRP1 expression. **B**, **C** Blood Pb concentration and brain regional Pb concentration following 4 weeks of Pb exposure. **D**, **E** Blood Pb concentration and brain regional Pb concentration following 8 weeks of Pb exposure. Data represent mean ± SD, n = 4–8; $^{*}p < 0.05$, $^{**}p < 0.01$, as compared to the controls; $^{\#}p < 0.05$, as compared to the low Pb exposure group. *ICA* internal carotid artery, *ECA* external carotid artery, *CCA* common carotid artery

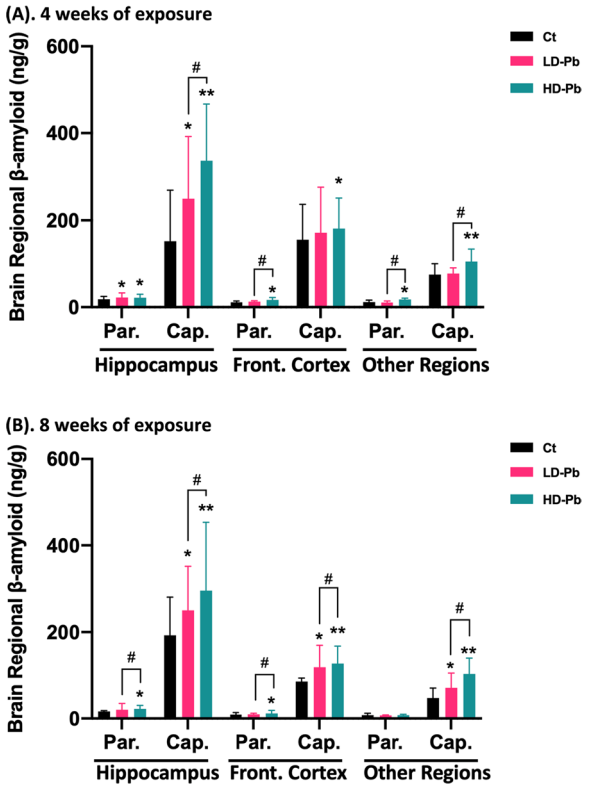

Fig. 3 Increased Aβ binding to cerebral capillaries following chronic in vivo Pb exposure. **A**, **B** Quantification of $A\beta_{40}$ concentration in cerebral parenchyma and capillaries following in situ brain perfusion of $A\beta_{40}$. Parenchymal and vascular fractions of specific brain regions were sampled from rats exposed to Pb (14 mg or 28 mg Pb/kg) and controls for 4 or 8 weeks. Data represent mean ± SD, n = 4–8; *$p < 0.05$, **$p < 0.01$, as compared to the controls in specific brain fraction; $^{\#}p < 0.05$ as compared to the low Pb exposure group in specific brain fraction. *Par.* parenchyma fraction, *Cap.* capillary fraction

for its clearance. Following 4 weeks of exposure, LRP1 expression in hippocampal parenchyma was significantly decreased by 48.7% and 64.1% in the low and high Pb exposure groups, respectively, as compared to controls ($p < 0.05$) (Fig. 4B), whereas its expression in hippocampal capillary did not change (Fig. 4A). Interestingly, Pb exposure significantly reduced LRP1 expression in the capillaries of frontal cortex by 45.5% and 67.0% in the low- and high-exposure groups, respectively, in comparison to controls ($p < 0.01$) (Fig. 4C). However, in the rest of tested fractions, i.e., hippocampal capillaries, frontal cortex parenchyma, and both fractions in other brain regions, no significant LRP1 expression alterations were found following the 4-week exposure (Fig. 4A, D–F).

Exposure to Pb for 8 weeks did not significantly alter LRP1 expression in all tested fractions except for the parenchyma collected from the rest of brain samples. There was a significantly downregulated LRP1 expression in the parenchyma of other brain regions, by 36.5% and 25.6% in the low- and high-Pb exposure groups, respectively ($p < 0.05$) (Fig. 4L). These Western blot data suggested that Pb-induced decline in LRP1 expression may contribute, at least in part, to the increased accumulation of $A\beta_{40}$ in cerebral vasculature and parenchyma.

Pb exposure disrupted LRP1 expression in hippocampal neurons and frontal cortex capillaries

The CA1, CA3, dentate gyrus (DG) of hippocampus and frontal cortex are specifically susceptible to vascular and parenchymal Aβ deposition [46, 66]. To study the expression of LRP1 as affected by Pb exposure in these subregions, we used IHC to co-stain LRP1 with CD31, a marker for endothelial cells, in rats following 4 weeks of low-dose in vivo Pb exposure. In hippocampal CA1, neurons expressed a high level of LRP1 in the perinuclear regions in control brains (Fig. 5A, A′), an observation consistent with reports elsewhere [1, 69]. Pb exposure significantly decreased neuronal LRP1 expression by 19.8% ($p < 0.01$) (Fig. 5A‴, B). Labeled by CD31 for cerebral vasculature, signals by LRP1 in control brains mostly surrounded CD31(+) capillaries, with a spatial proximity observed between LRP1 and CD31 signals (Fig. 5A″). Pb exposure, however, caused a discontinuous LRP1 expression around CD31(+) endothelium and the dissociation of LRP1 from CD31 (Fig. 5A⁗). Nevertheless, the fluorescent intensity of LRP1 in CA1 capillaries was not significantly altered (Fig. 5B).

LRP1 in CA3 was highly enriched in neuronal cells in the control group, showing a strong perinuclear expression pattern (Fig. 5C′) similar to the CA1 region (Fig. 5A′). Pb exposure significantly decreased LRP1 expression in CA3 neuronal cells by 34.8% (Fig. 5C‴, D). Similar to the Pb-exposed CA1 region, LRP1 in CA3 capillaries of Pb-treated rats was discontinuous from CD31(+) endothelium (Fig. 5C⁗). Additionally, a LRP1-CD31 signal separation, i.e., a gap existing between LRP1

(See figure on next page.)

Fig. 4 Altered LRP1 expression in brain capillary and parenchyma fractions following 4 or 8 weeks of in vivo Pb exposure in rats. **A**–**F** Effects of 4-week Pb exposure on LRP1 expression in hippocampal capillaries (**A**), hippocampal parenchyma (**B**), frontal cortex capillaries (**C**), frontal cortex parenchyma (**D**), capillaries of other brain regions (**E**), and parenchyma of other brain regions (**F**) by Western blot (WB). **G**–**L** Effects of 8-week Pb exposure on LRP1 expression in hippocampal capillaries (**G**), hippocampal parenchyma (**H**), frontal cortex capillaries (**I**), frontal cortex parenchyma (**J**), capillaries of other brain regions (**K**), and parenchyma of other brain regions (**L**) by WB. Data represent mean ± SD, n = 3; *$p < 0.05$ and **$p < 0.01$, as compared to the controls in specific brain fraction

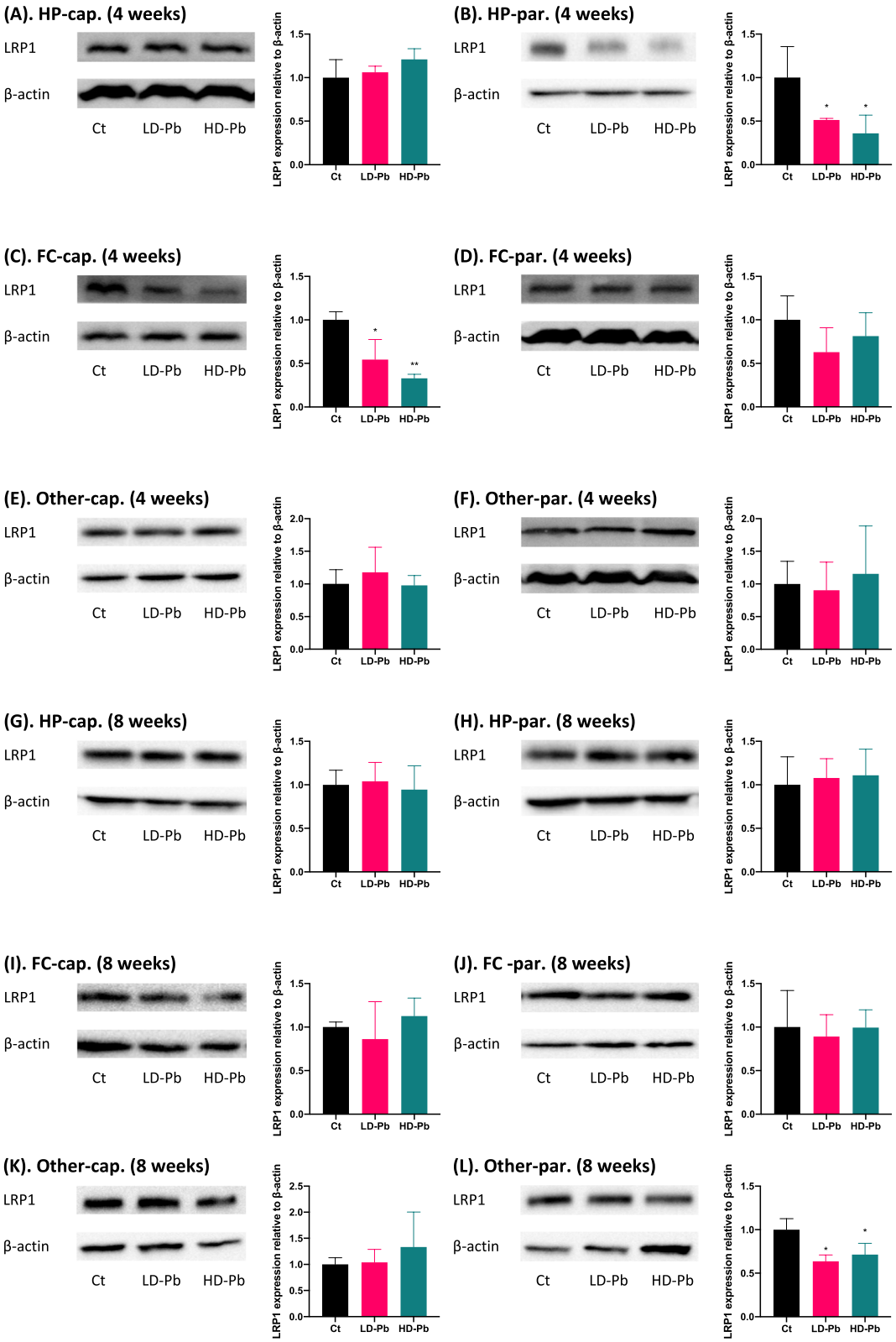

Fig. 4 (See legend on previous page.)

and CD31, was observed in Pb-exposed animals but rarely in controls. Yet, quantitative analyses of LRP1 fluorescent intensity in CA3 vasculature did not yield a significant difference (Fig. 5D).

LRP1 in the control DG was abundantly expressed by the local neuronal cells in the perinuclear areas (Fig. 5E′). Nevertheless, its expression was significantly reduced by 35.9% by Pb exposure ($p < 0.01$) (Fig. 5E‴, F). In DG vasculature, LRP1 expressed along CD31(+) capillaries remained to be continuous and strong in controls (Fig. 5E″); but Pb exposure seemed to disperse LRP1 signals around the CD31-expressing vascular cells (Fig. 5E⁗). However, quantitative analysis of LRP1 expression by the fluorescent intensity did not show significant changes in DG capillaries between groups (Fig. 5F).

Expression of LRP1 in the frontal cortex exhibited a gradient pattern with the signal intensity declining gradually from the dorsal area (closer to the pial surface; pial.) towards the ventral (the corpus callosum; CC) (Fig. 5G). In neuronal cells with the typical perinuclear distribution, LRP1 level was not significantly changed by Pb exposure (Fig. 5G, H). However, Pb exposure not only disrupted LRP1 distribution around the cortical vasculature but also decreased LRP1 expression (Fig. 5G, H).

Overall, through characterizing the LRP1 expression in specific brain subregions/fractions, our data showed that this $A\beta_{40}$ transporting protein was adversely affected by Pb exposure.

Discussion

Our findings revealed a strikingly high affinity of $A\beta_{40}$ to cerebral capillaries, which was characterized by (1) a short time 2-min perfusion leading to $A\beta_{40}$ accumulation; (2) the ability of the cerebral capillary in sequestering $A\beta_{40}$ molecules far more than brain parenchyma in all tested brain regions; and (3) a high affinity of $A\beta_{40}$ to the capillaries in hippocampus and frontal cortex. The exact mechanism by which $A\beta_{40}$ accumulates in cerebral capillary is unknown. The initial binding of $A\beta_{40}$ to cerebral capillaries, regardless of the subsequent biological events (transcytosis, exocytosis, or degradation), is largely dependent upon the cell-surface receptors; the subsequent receptor-mediated endocytosis occurs allowing for the $A\beta_{40}$ uptake [30, 47]. Receptors critical to $A\beta_{40}$ uptake such as RAGE, P-glycoprotein, integrins and scavenger receptors, etc., are known to express highly in the cerebral vasculature [68, 73]. This may explain partly of the high affinity of Aβ to cerebral endothelia following in situ perfusion. In addition, one of the pathways to eliminate cerebrovascular Aβ is via a perivascular drainage system transporting Aβ alongside the vascular wall. On the way entering this drainage system, Aβ molecules may polymerize into fibrils on vascular basement membrane by interacting with extracellular components, enabling excessive Aβ accumulation [70]. However, questions remain as to where Aβ molecules accumulate the surface of blood-facing endothelia, within the endothelial cytosol, and/or between basolateral endothelium and vascular smooth muscular layer, and whether cerebral endothelial cells possess the unique binding site(s) for Aβ molecules as compared to other peripheral endothelial cell types. Thus, our observation calls for more research in the future to uncover the mechanism underlying the high affinity of $A\beta_{40}$ to the cerebral vasculature.

Pb exposure, either in vitro or in vivo, evidently increased the deposition of $A\beta_{40}$ in cerebral capillary; both hippocampus and brain cortex appeared to sequester more $A\beta_{40}$ than other brain regions. The status of Aβ in the cerebral vasculature is regulated by several coordinated processes, including the influx on the endothelial cell surface as discussed above, intracellular degradation, and/or the efflux or removal of Aβ by the BBB. Interestingly, cell-surface integrin, a molecule responsible for Aβ adhesion and uptake, can be upregulated in vasculature upon inflammation [35], a condition frequently reported in Pb-induced neurotoxicity [6]. A recent report also shows that a compromised BBB integrity, a typical neurotoxicity associated with Pb exposure [21, 56, 63], can aggravate the vascular $A\beta_{40}$ accumulation [62]. It is, thus, highly possible that chronic Pb exposure in the current study may cause the damage to the BBB, which in turn exacerbates the Aβ-capillary binding. Since the high affinity of $A\beta_{40}$ to cerebral capillaries is due to surface

(See figure on next page.)

Fig. 5 LRP1 expression in neurons and capillaries in hippocampal subfields and frontal cortex following 4 weeks of lose-dose in vivo Pb exposure. **A** IHC staining of hippocampal CA1 region with LRP1 and CD31. LRP1 expression in CA1 neurons (A′ and A‴) and capillaries (A″ and A⁗) were further magnified in panels below. **B** Quantification of LRP1 expression by fluorescent intensity in neurons and capillaries in hippocampal CA1 region. **C** IHC staining of hippocampal CA3 region with LRP1 and CD31. LRP1 expression in CA3 neurons (C′ and C‴) and capillaries (C″ and C⁗) were further magnified in panels below. **D** Quantification of LRP1 fluorescent intensity in neurons and capillaries in hippocampal CA3 region. **E** IHC staining of hippocampal dentate gyrus (DG) with LRP1 and CD31. LRP1 expression in DG neurons (E′ and E‴) and capillaries (E″ and E⁗) were further magnified in panels below. **F** Quantification of LRP1 expression by fluorescent intensity in neurons and capillaries in hippocampal DG. **G** IHC staining of frontal cortex region with LRP1 and CD31. Pial surface (Pial.) and corpus callosum (CC) were labeled to show LRP1 expression pattern. Selected regions were further magnified to show LRP1 expression in cortical neurons and capillaries as affected by Pb exposure. **H** Quantification of LRP1 expression by immunofluorescent intensity in neurons and capillaries in frontal cortex. Data represent mean ± SD, n = 4; $^{**}p < 0.01$, as compared to the controls in the specific fraction

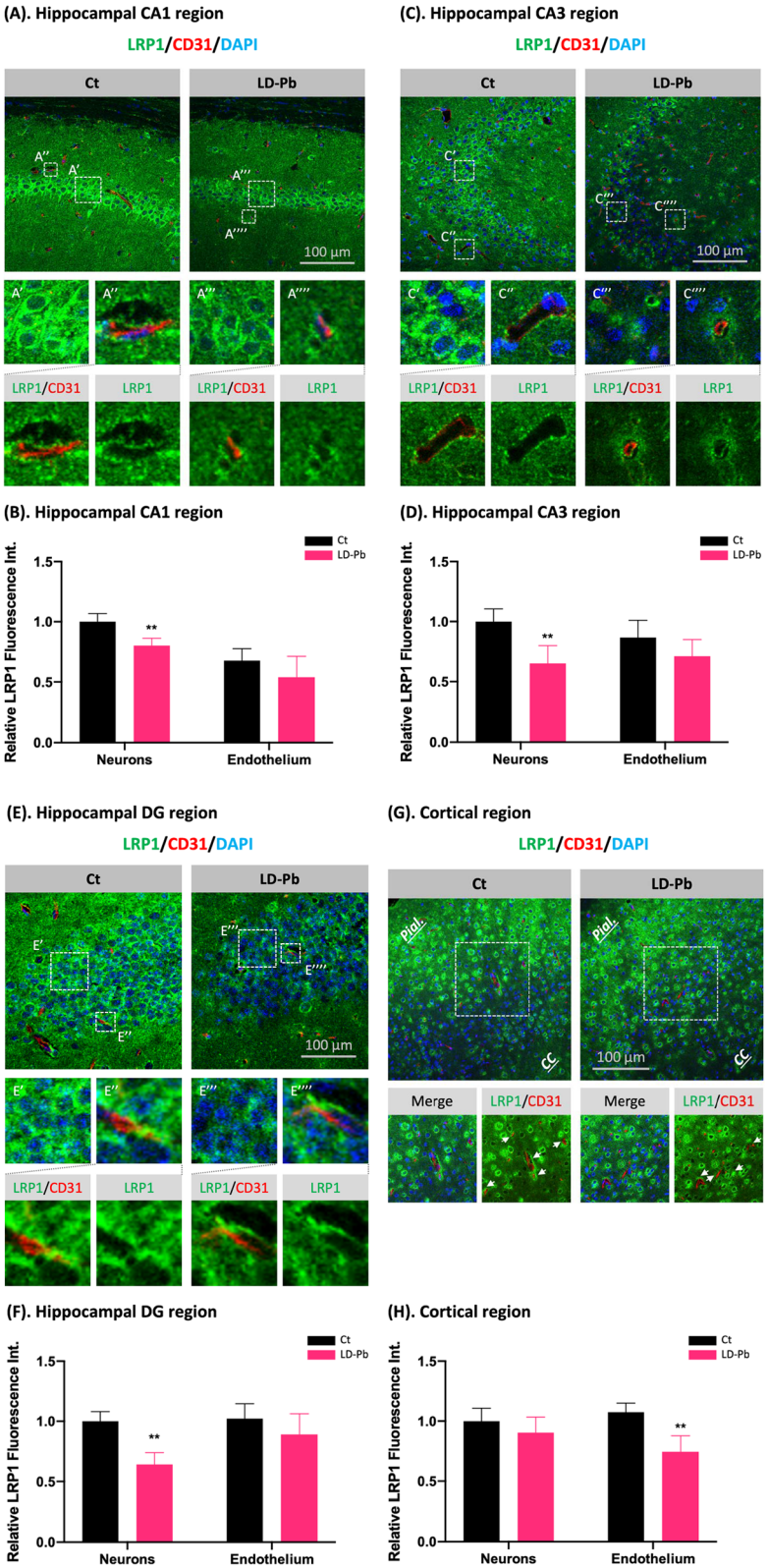

Fig. 5 (See legend on previous page.)

binding, intracellular uptake, or both, immunogold labeling of Aβ with electron microscopy is needed to explain this high affinity by characterizing the subcellular location of Aβ [54]. Alternatively, stimulated emission depletion (STED) microscopic technique, which provides superior imaging performance, can be utilized for the same purpose: colocalization of Aβ with endothelial luminal markers such as carbonic anhydrase IV (CA IV) [18] would differentiate the "binding" and "uptake".

A defection in Aβ clearance represents another theory in pathological mechanism for AD [17, 29, 37, 44, 57, 65]. Routes to clear Aβ in the central nervous system involve receptor-mediated clearance through the BBB [10], interstitial fluid bulk flow through the perivascular/glymphatic system [27, 64], and absorption from the CSF through the choroid plexus [52]. In the BBB system, Aβ is mainly cleared by a LRP1-mediated efflux [29, 45, 55, p. 1]. Conditional knockdown of LRP1 in cerebral endothelial and vascular smooth muscle cells significantly accelerates the cognitive and memory deficits by exacerbating the formation of Aβ plaque and CAA in transgenic mice [29, 55]. The current study showed a Pb-induced decline of LRP1 expression, specifically in cortical capillaries, where the CAA often develops. In addition, in the Pb-exposed hippocampus, LRP1, which normally expressed continuously along the endothelia in controls, distributed abnormally in a discontinuous patten, suggesting a defective Aβ clearance [53, 55].

Noticeably also, reports in literature indicate that Aβ drainage occurs as interstitial fluid bulk flow via the perivascular space along the cerebral vasculature, and in the due process, aquaporin 4 (AQP4) transporter expressed on astrocytes determines the perivascular/glymphatic drainage [23]. Interestingly Pb exposure disrupts AQP4 expression and function [23]. The current study does not address Pb toxicity towards astrocytes and AQP4; yet this line of study deserves attention for further investigation. In addition, the choroid plexus (CP), despite its bidirectionality for Aβ transport, selectively effluxes Aβ from the CSF-facing to the blood-facing side [8]; however, Pb exposure impairs LRP1-associated Aβ efflux mechanism at the choroid plexus [22, 52, 69], which may contribute to the brain Aβ overload. The meningeal system also facilitates the Aβ efflux through the lymphatics vessels [9], but its susceptibility to Pb toxicity remains elusive. Overall, we propose that multiple overlapping or interactive Aβ removal mechanisms may collectively account for Pb-induced Ab accumulation in brain.

LRP1 is not solely expressed in cerebral vasculature but also present abundantly in neurons [34]; its presence promotes neuronal cell survival, axon growth, and neurite outgrowth [15, 16, 71]. Our data by IHC and WB indicated that in vivo Pb exposure specifically decreased LRP1 in hippocampal but not cortical neurons. This observation suggested that memory-related symptoms present in Pb-exposed populations or experimental animals could be, at least in part, caused by a decreased LRP1 expression in neuronal cells in these areas. Indeed, the use of pioglitazone, a peroxisome proliferator activated receptor-γ (PPAR-γ) agonist known to increase LRP1 in the brain, significantly ameliorated the learning and memory impairment in AD transgenic mice by upregulating neuronal LRP1 expression in hippocampal neurons [50]. Thus, the degree to which the decreased neuronal LRP1 expression may contribute to Pb-induced neurotoxicity including learning deficits deserves further testing.

The current study has two limitations. First, there was an apparent discrepancy between the increased hippocampal and cortical capillary Aβ accumulation and the altered LRP1 expression. While Aβ molecules continued to accumulate in brain capillary fractions after 8-week chronic Pb exposure, LRP1 expression was not significantly altered in these brain fractions except for the parenchyma fraction of the rest of brain. It is possible that Pb may dysregulate the expression of RAGE at BBB as it did in the blood–CSF barrier in the choroid plexus [52]. An increased RAGE in the choroid plexus following 8-week Pb exposure underlies an increased Ab uptake by the choroid plexus [52]. Similarly, increased Ab levels in the cerebral vasculature could be due to Pb-induced expression of RAGE in the BBB. Thus, the effect of chronic Pb exposure on many other Ab transporting proteins in the BBB deserves future exploration. In addition, Pb exposure is known to damage the cerebral vasculature [41, 43, 60]. Noticeably also, brain endothelial cells are regionally heterogenous, rendering them more diverse in response to Pb exposure [5], this regional heterogeneity is even greater in neuronal cells [72]. Hence, it is possible that the spatial cellular heterogeneity also contributed to LRP1 alterations in the frontal cortex capillaries and hippocampal parenchyma by Pb, but not in others.

This study, due to the limited resource in the original experimental design, did not explicitly examine the relationship between BBB injury and Ab accumulation. Thus, it is desirable to conduct histopathological experiments to verify how the altered BBB integrity following Pb exposure may facilitate binding of Ab molecules to cerebral vasculature in our future experiments.

In summary, the current study demonstrates that the cerebral vasculature naturally possesses a strikingly high affinity to Aβ present in circulating blood; Pb exposure, either in vitro or in vivo greatly increases Aβ accumulation in cerebral vasculature. Such an increased Aβ buildup is due partly to the diminished expression of an

Aβ efflux carrier LRP1 in response to Pb in tested brain region and fractions. Mechanisms underlying these alterations and the relationship to the development Pb-induced AD deserve further experimental testing.

Supplementary Information

The online version contains supplementary material available at https://doi.org/10.1186/s12987-023-00432-5.

Additional file 1: Figure S1. Negative control staining for immunohistochemistry experiments.

Acknowledgements
The authors thank Dr. Jason R. Cannon at Purdue University for making the microtome available. Graphical illustrations in this study were created with BioRender.com.

Author contributions
Conceptualization: WZ, XS, LLL; methodology: XS, LLL, GH, WZ; investigation: LLL, XS, GH, WZ; writing—original draft: LLL; writing—review and editing: WZ, LLL; funding acquisition: WZ, DY; resources: WZ, DY; supervision: WZ, DY. All authors have agreed to the published version of the manuscript. All authors read and approved the final manuscript.

Funding
This study was supported by U.S. National Institute of Health (NIH)/National Institute of Environmental Health Sciences (NIEHS) Grants Number R01 ES027078 (WZ and YD).

Availability of data and materials
Not applicable.

Declarations

Ethics approval and consent to participate
Not applicable.

Consent for publication
We, the undersigned co-authors, give our consent for the publication of identifiable details, which include figures, tables, and details within the text to be published in FBCNS.

Competing interests
The authors declare that they have no competing interests.

Author details
[1]School of Health Sciences, Purdue University, 550 Stadium Mall Drive, HAMP-1273, West Lafayette, IN 47907, USA. [2]School of Public Health, Qingdao University, Qingdao, China. [3]Department of Neurology, Indiana University School of Medicine, Indianapolis, IN, USA. [4]Department of Medical Biology, School of Basic Medical Sciences, Hubei University of Chinese Medicine, Wuhan, China.

Received: 9 December 2022 Accepted: 10 April 2023
Published online: 01 May 2023

References

1. Auderset L, Cullen CL, Young KM. Low density lipoprotein-receptor related protein 1 is differentially expressed by neuronal and glial populations in the developing and mature mouse central nervous system. PLoS ONE. 2016;11: e0155878. https://doi.org/10.1371/journal.pone.0155878.
2. Banerjee G, Adams ME, Jaunmuktane Z, Alistair Lammie G, Turner B, Wani M, Sawhney IMS, Houlden H, Mead S, Brandner S, Werring DJ. Early onset cerebral amyloid angiopathy following childhood exposure to cadaveric dura: Banerjee: early onset CAA. Ann Neurol. 2019;85:284–90. https://doi.org/10.1002/ana.25407.
3. Behl M, Zhang Y, Monnot AD, Jiang W, Zheng W. Increased β-amyloid levels in the choroid plexus following lead exposure and the involvement of low-density lipoprotein receptor protein-1. Toxicol Appl Pharmacol. 2009;240:245–54. https://doi.org/10.1016/j.taap.2009.05.024.
4. Benedikz E, Kloskowska E, Winblad B. The rat as an animal model of Alzheimer's disease. J Cell Mol Med. 2009;13:1034–42. https://doi.org/10.1111/j.1582-4934.2009.00781.x.
5. Bryant A, Li Z, Jayakumar R, Serrano-Pozo A, Woost B, Hu M, Woodbury ME, Wachter A, Lin G, Kwon T, Talanian RV, Biber K, Karran EH, Hyman BT, Das S, Bennett R. Endothelial cells are heterogeneous in different brain regions and are dramatically altered in Alzheimer's disease. bioRxiv. 2023. https://doi.org/10.1101/2023.02.16.528825.
6. Chibowska K, Baranowska-Bosiacka I, Falkowska A, Gutowska I, Goschorska M, Chlubek D. Effect of lead (Pb) on inflammatory processes in the brain. IJMS. 2016;17:2140. https://doi.org/10.3390/ijms17122140.
7. Choi BS, Zheng W. Copper transport to the brain by the blood–brain barrier and blood–CSF barrier. Brain Res. 2009. https://doi.org/10.1016/j.brainres.2008.10.056.
8. Crossgrove JS, Li GJ, Zheng W. The choroid plexus removes β-amyloid from brain cerebrospinal fluid. Exp Biol Med (Maywood). 2005;230:771–6. https://doi.org/10.1177/153537020523001011.
9. Da Mesquita S, Louveau A, Vaccari A, Smirnov I, Cornelison RC, Kingsmore KM, Contarino C, Onengut-Gumuscu S, Farber E, Raper D, Viar KE, Powell RD, Baker W, Dabhi N, Bai R, Cao R, Hu S, Rich SS, Munson JM, Lopes MB, Overall CC, Acton ST, Kipnis J. Functional aspects of meningeal lymphatics in ageing and Alzheimer's disease. Nature. 2018;560:185–91. https://doi.org/10.1038/s41586-018-0368-8.
10. Deane R, Bell R, Sagare A, Zlokovic B. Clearance of amyloid-β peptide across the blood–brain barrier: implication for therapies in Alzheimers disease. CNSNDDT. 2009;8:16–30. https://doi.org/10.2174/187152709787601867.
11. Deane R, Du Yan S, Submamaryan RK, LaRue B, Jovanovic S, Hogg E, Welch D, Manness L, Lin C, Yu J, Zhu H, Ghiso J, Frangione B, Stern A, Schmidt AM, Armstrong DL, Arnold B, Liliensiek B, Nawroth P, Hofman F, Kindy M, Stern D, Zlokovic B. RAGE mediates amyloid-β peptide transport across the blood–brain barrier and accumulation in brain. Nat Med. 2003;9:907–13. https://doi.org/10.1038/nm890.
12. Deane R, Zheng W, Zlokovic BV. Brain capillary endothelium and choroid plexus epithelium regulate transport of transferrin-bound and free iron into the rat brain: iron transport at the CNS barriers. J Neurochem. 2004;88:813–20. https://doi.org/10.1046/j.1471-4159.2003.02221.x.
13. Donahue JE, Flaherty SL, Johanson CE, Duncan JA, Silverberg GD, Miller MC, Tavares R, Yang W, Wu Q, Sabo E, Hovanesian V, Stopa EG. RAGE, LRP-1, and amyloid-beta protein in Alzheimer's disease. Acta Neuropathol. 2006;112:405–15. https://doi.org/10.1007/s00401-006-0115-3.
14. Fu X, Zhang Y, Jiang W, Monnot AD, Bates CA, Zheng W. Regulation of copper transport crossing brain barrier systems by CU-ATPases: effect of manganese exposure. Toxicol Sci. 2014. https://doi.org/10.1093/toxsci/kfu048.
15. Fuentealba RA, Liu Q, Kanekiyo T, Zhang J, Bu G. Low density lipoprotein receptor-related protein 1 promotes anti-apoptotic signaling in neurons by activating Akt survival pathway. J Biol Chem. 2009;284:34045–53. https://doi.org/10.1074/jbc.M109.021030.
16. García-Fernández P, Üçeyler N, Sommer C. From the low-density lipoprotein receptor-related protein 1 to neuropathic pain: a potentially novel target. PR9. 2021;6: e898. https://doi.org/10.1097/PR9.0000000000000898.
17. Gatti L, Tinelli F, Scelzo E, Arioli F, Di Fede G, Obici L, Pantoni L, Giaccone G, Caroppo P, Parati EA, Bersano A. Understanding the pathophysiology of cerebral amyloid angiopathy. IJMS. 2020;21:3435. https://doi.org/10.3390/ijms21103435.
18. Ghandour MS, Langley OK, Zhu XL, Waheed A, Sly WS. Carbonic anhydrase IV on brain capillary endothelial cells: a marker associated with the blood–brain barrier. Proc Natl Acad Sci USA. 1992;89:6823–7. https://doi.org/10.1073/pnas.89.15.6823.
19. Graves AB, Van Duijn CM, Chandra V, Fratiglioni L, Heyman A, Jorm AF, Kokmen E, Kondo K, Mortimer JA, Rocca WA, Shalat SL, Soininen H, A Hofman for the Eurodem Risk Factors Research Group. Occupational exposures to solvents and lead as risk factors for Alzheimer's disease:

a collaborative re-analysis of case-control studies. Int J Epidemiol. 1991;20:S58–61. https://doi.org/10.1093/ije/20.Supplement_2.S58.
20. Gu H, Robison G, Hong L, Barrea R, Wei X, Farlow MR, Pushkar YN, Du Y, Zheng W. Increased β-amyloid deposition in Tg-SWDI transgenic mouse brain following in vivo lead exposure. Toxicol Lett. 2012;213:211–9. https://doi.org/10.1016/j.toxlet.2012.07.002.
21. Gu H, Territo PR, Persohn SA, Bedwell AA, Eldridge K, Speedy R, Chen Z, Zheng W, Du Y. Evaluation of chronic lead effects in the blood brain barrier system by DCE-CT. J Trace Elem Med Biol. 2020;62: 126648. https://doi.org/10.1016/j.jtemb.2020.126648.
22. Gu H, Wei X, Monnot AD, Fontanilla CV, Behl M, Farlow MR, Zheng W, Du Y. Lead exposure increases levels of β-amyloid in the brain and CSF and inhibits LRP1 expression in APP transgenic mice. Neurosci Lett. 2011;490:16–20. https://doi.org/10.1016/j.neulet.2010.12.017.
23. Gunnarson E, Axehult G, Baturina G, Zelenin S, Zelenina M, Aperia A. Lead induces increased water permeability in astrocytes expressing aquaporin 4. Neuroscience. 2005;136:105–14. https://doi.org/10.1016/j.neuroscience.2005.07.027.
24. Haraguchi T, Ishizu H, Takehisa Y, Kawai K, Yokota O, Terada S, Tsuchiya K, Ikeda K, Morita K, Horike T, Kira S, Kuroda S. Lead content of brain tissue in diffuse neurofibrillary tangles with calcification (DNTC): the possibility of lead neurotoxicity. NeuroReport. 2001;12:3887–90. https://doi.org/10.1097/00001756-200112210-00006.
25. Hossain MA, Russell JC, Miknyoczki S, Ruggeri B, Lal B, Laterra J. Vascular endothelial growth factor mediates vasogenic edema in acute lead encephalopathy. Ann Neurol. 2004;55:660–7. https://doi.org/10.1002/ana.20065.
26. Humpel C. Identifying and validating biomarkers for Alzheimer's disease. Trends Biotechnol. 2011;29:26–32. https://doi.org/10.1016/j.tibtech.2010.09.007.
27. Iliff JJ, Wang M, Liao Y, Plogg BA, Peng W, Gundersen GA, Benveniste H, Vates GE, Deane R, Goldman SA, Nagelhus EA, Nedergaard M. A paravascular pathway facilitates CSF flow through the brain parenchyma and the clearance of interstitial solutes, including amyloid β. Sci Transl Med. 2012. https://doi.org/10.1126/scitranslmed.3003748.
28. Jaunmuktane Z, Mead S, Ellis M, Wadsworth JDF, Nicoll AJ, Kenny J, Launchbury F, Linehan J, Richard-Loendt A, Walker AS, Rudge P, Collinge J, Brandner S. Evidence for human transmission of amyloid-β pathology and cerebral amyloid angiopathy. Nature. 2015;525:247–50. https://doi.org/10.1038/nature15369.
29. Kanekiyo T, Liu C-C, Shinohara M, Li J, Bu G. LRP1 in brain vascular smooth muscle cells mediates local clearance of Alzheimer's amyloid. J Neurosci. 2012;32:16458–65. https://doi.org/10.1523/JNEUROSCI.3987-12.2012.
30. Lai AY, McLaurin J. Mechanisms of amyloid-beta peptide uptake by neurons: the role of lipid rafts and lipid raft-associated proteins. Int J Alzheimer's Dis. 2011;2011:1–11. https://doi.org/10.4061/2011/548380.
31. Liu LL, Du D, Zheng W, Zhang Y. Age-dependent decline of copper clearance at the blood-cerebrospinal fluid barrier. Neurotoxicology. 2022;88:44–56. https://doi.org/10.1016/j.neuro.2021.10.011.
32. Bakulski KM, Rozek LS, Dolinoy DC, Paulson HL, Hu H. Alzheimer's disease and environmental exposure to lead: the epidemiologic evidence and potential role of epigenetics. CAR. 2012;9:563–73. https://doi.org/10.2174/156720512800617991.
33. Mattson M, Cheng B, Davis D, Bryant K, Lieberburg I, Rydel R. beta-Amyloid peptides destabilize calcium homeostasis and render human cortical neurons vulnerable to excitotoxicity. J Neurosci. 1992;12:376–89. https://doi.org/10.1523/JNEUROSCI.12-02-00376.1992.
34. May P, Rohlmann A, Bock HH, Zurhove K, Marth JD, Schomburg ED, Noebels JL, Beffert U, Sweatt JD, Weeber EJ, Herz J. Neuronal LRP1 functionally associates with postsynaptic proteins and is required for normal motor function in mice. Mol Cell Biol. 2004;24:8872–83. https://doi.org/10.1128/MCB.24.20.8872-8883.2004.
35. Mezu-Ndubuisi OJ, Maheshwari A. The role of integrins in inflammation and angiogenesis. Pediatr Res. 2021;89:1619–26. https://doi.org/10.1038/s41390-020-01177-9.
36. Niklowitz WJ, Mandybur TI. Neurofibrillary changes following childhood lead encephalopathy: case report. J Neuropathol Exp Neurol. 1975;34:445–55. https://doi.org/10.1097/00005072-197509000-00006.
37. Nikolakopoulou AM, Wang Y, Ma Q, Sagare AP, Montagne A, Huuskonen MT, Rege SV, Kisler K, Dai Z, Körbelin J, Herz J, Zhao Z, Zlokovic BV. Endothelial LRP1 protects against neurodegeneration by blocking cyclophilin A. J Exp Med. 2021;218: e20202207. https://doi.org/10.1084/jem.20202207.
38. Oakley H, Cole SL, Logan S, Maus E, Shao P, Craft J, Guillozet-Bongaarts A, Ohno M, Disterhoft J, Van Eldik L, Berry R, Vassar R. Intraneuronal β-amyloid aggregates, neurodegeneration, and neuron loss in transgenic mice with five familial Alzheimer's disease mutations: potential factors in amyloid plaque formation. J Neurosci. 2006;26:10129–40. https://doi.org/10.1523/JNEUROSCI.1202-06.2006.
39. Osgood D, Miller MC, Messier AA, Gonzalez L, Silverberg GD. Aging alters mRNA expression of amyloid transporter genes at the blood–brain barrier. Neurobiol Aging. 2017;57:178–85. https://doi.org/10.1016/j.neurobiolaging.2017.05.011.
40. Pardridge WM. The isolated brain microvessel: a versatile experimental model of the blood–brain barrier. Front Physiol. 2020;11:398. https://doi.org/10.3389/fphys.2020.00398.
41. Press MF. Lead encephalopathy in neonatal long-evans rats: morphologic studies. J Neuropathol Exp Neurol. 1977;36:169–93. https://doi.org/10.1097/00005072-197701000-00014.
42. Price DL, Sisodia SS, Borchelt DR. Genetic neurodegenerative diseases: the human illness and transgenic models. Science. 1998;282:1079–83. https://doi.org/10.1126/science.282.5391.1079.
43. Prozialeck WC, Edwards JR, Nebert DW, Woods JM, Barchowsky A, Atchison WD. The vascular system as a target of metal toxicity. Toxicol Sci. 2008;102:207–18. https://doi.org/10.1093/toxsci/kfm263.
44. Qi X, Ma J. The role of amyloid beta clearance in cerebral amyloid angiopathy: more potential therapeutic targets. Transl Neurodegener. 2017;6:22. https://doi.org/10.1186/s40035-017-0091-7.
45. Ramanathan A, Nelson AR, Sagare AP, Zlokovic BV. Impaired vascular-mediated clearance of brain amyloid beta in Alzheimer's disease: the role, regulation and restoration of LRP1. Front Aging Neurosci. 2015. https://doi.org/10.3389/fnagi.2015.00136.
46. Reilly JF, Games D, Rydel RE, Freedman S, Schenk D, Young WG, Morrison JH, Bloom FE. Amyloid deposition in the hippocampus and entorhinal cortex: quantitative analysis of a transgenic mouse model. Proc Natl Acad Sci USA. 2003;100:4837–42. https://doi.org/10.1073/pnas.0330745100.
47. Ries M, Sastre M. Mechanisms of Aβ clearance and degradation by glial cells. Front Aging Neurosci. 2016. https://doi.org/10.3389/fnagi.2016.00160.
48. Schwartz BS, Caffo B, Stewart WF, Hedlin H, James BD, Yousem D, Davatzikos C. Evaluation of cumulative lead dose and longitudinal changes in structural magnetic resonance imaging in former organolead workers. J Occup Environ Med. 2010;52:407–14. https://doi.org/10.1097/JOM.0b013e3181d5e386.
49. Selkoe DJ. Biochemistry of altered brain proteins in Alzheimer's disease. Annu Rev Neurosci. 1989;12:463–90. https://doi.org/10.1146/annurev.ne.12.030189.002335.
50. Seok H, Lee M, Shin E, Yun MR, Lee Y, Moon JH, Kim E, Lee PH, Lee B-W, Kang ES, Lee HC, Cha BS. Low-dose pioglitazone can ameliorate learning and memory impairment in a mouse model of dementia by increasing LRP1 expression in the hippocampus. Sci Rep. 2019;9:4414. https://doi.org/10.1038/s41598-019-40736-x.
51. Seubert P, Vigo-Pelfrey C, Esch F, Lee M, Dovey H, Davis D, Sinha S, Schiossmacher M, Whaley J, Swindlehurst C, McCormack R, Wolfert R, Selkoe D, Lieberburg I, Schenk D. Isolation and quantification of soluble Alzheimer's β-peptide from biological fluids. Nature. 1992;359:325–7. https://doi.org/10.1038/359325a0.
52. Shen X, Xia L, Liu L, Jiang H, Shannahan J, Du Y, Zheng W. Altered clearance of beta-amyloid from the cerebrospinal fluid following subchronic lead exposure in rats: roles of RAGE and LRP1 in the choroid plexus. J Trace Elem Med Biol. 2020. https://doi.org/10.1016/j.jtemb.2020.126520.
53. Silverberg GD, Messier AA, Miller MC, Machan JT, Majmudar SS, Stopa EG, Donahue JE, Johanson CE. Amyloid efflux transporter expression at the blood–brain barrier declines in normal aging. J Neuropathol Exp Neurol. 2010;69:1034–43. https://doi.org/10.1097/NEN.0b013e3181f46e25.
54. Skaaraas GHES, Melbye C, Puchades MA, Leung DSY, Jacobsen Ø, Rao SB, Ottersen OP, Leergaard TB, Torp R. Cerebral amyloid angiopathy in a mouse model of Alzheimer's disease associates with upregulated angiopoietin and downregulated hypoxia-inducible factor. JAD. 2021;83:1651–63. https://doi.org/10.3233/JAD-210571.
55. Storck SE, Meister S, Nahrath J, Meißner JN, Schubert N, Di Spiezio A, Baches S, Vandenbroucke RE, Bouter Y, Prikulis I, Korth C, Weggen S,

Heimann A, Schwaninger M, Bayer TA, Pietrzik CU. Endothelial LRP1 transports amyloid-β1-42 across the blood–brain barrier. J Clin Investig. 2015;126:123–36. https://doi.org/10.1172/JCI81108.
56. Strużyńska L, Walski M, Gadamski R, Dabrowska-Bouta B, Rafałowska U. Lead-induced abnormalities in blood–brain barrier permeability in experimental chronic toxicity. Mol Chem Neuropathol. 1997;31:207–24. https://doi.org/10.1007/BF02815125.
57. Tarasoff-Conway JM, Carare RO, Osorio RS, Glodzik L, Butler T, Fieremans E, Axel L, Rusinek H, Nicholson C, Zlokovic BV, Frangione B, Blennow K, Ménard J, Zetterberg H, Wisniewski T, de Leon MJ. Clearance systems in the brain—implications for Alzheimer disease. Nat Rev Neurol. 2015;11:457–70. https://doi.org/10.1038/nrneurol.2015.119.
58. Toews AD, Kolber A, Hayward J, Krigman MR, Morell P. Experimental lead encephalopathy in the suckling rat: concentration of lead in cellular fractions enriched in brain capillaries. Brain Res. 1978;147:131–8. https://doi.org/10.1016/0006-8993(78)90777-1.
59. Tsoi MF, Lo CWH, Cheung TT, Cheung BMY. Blood lead level and risk of hypertension in the United States National Health and nutrition examination survey 1999–2016. Sci Rep. 2021;11:3010. https://doi.org/10.1038/s41598-021-82435-6.
60. Vaziri ND. Mechanisms of lead-induced hypertension and cardiovascular disease. Am J Physiol Heart Circ Physiol. 2008;295:H454–65. https://doi.org/10.1152/ajpheart.00158.2008.
61. Vigo-Pelfrey C, Lee D, Keim P, Lieberburg I, Schenk DB. Rapid communication: characterization of β-amyloid peptide from human cerebrospinal fluid. J Neurochem. 1993;61:1965–8. https://doi.org/10.1111/j.1471-4159.1993.tb09841.x.
62. Wang D, Chen F, Han Z, Yin Z, Ge X, Lei P. Relationship between amyloid-β deposition and blood–brain barrier dysfunction in Alzheimer's disease. Front Cell Neurosci. 2021;15: 695479. https://doi.org/10.3389/fncel.2021.695479.
63. Wang Q, Luo W, Zheng W, Liu Y, Xu H, Zheng G, et al. Iron supplement prevents lead-induced disruption of the blood–brain barrier during rat development. Toxicol Appl Pharmacol. 2007;219:33–41. https://doi.org/10.1016/j.taap.2006.11.035
64. Weller RO, Subash M, Preston SD, Mazanti I, Carare RO. SYMPOSIUM: clearance of Aβ from the brain in Alzheimer's disease: perivascular drainage of amyloid-β peptides from the brain and its failure in cerebral amyloid angiopathy and Alzheimer's disease: perivascular drainage of aβ peptides and cerebral amyloid angiopathy. Brain Pathol. 2007;18:253–66. https://doi.org/10.1111/j.1750-3639.2008.00133.x.
65. Wildsmith KR, Holley M, Savage JC, Skerrett R, Landreth GE. Evidence for impaired amyloid β clearance in Alzheimer's disease. Alzheimers Res Ther. 2013;5:33. https://doi.org/10.1186/alzrt187.
66. Willumsen N, Poole T, Nicholas JM, Fox NC, Ryan NS, Lashley T. Variability in the type and layer distribution of cortical Aβ pathology in familial Alzheimer's disease. Brain Pathol. 2022. https://doi.org/10.1111/bpa.13009.
67. Wu J, Basha MdR, Brock B, Cox DP, Cardozo-Pelaez F, McPherson CA, Harry J, Rice DC, Maloney B, Chen D, Lahiri DK, Zawia NH. Alzheimer's disease (AD)-like pathology in aged monkeys after infantile exposure to environmental metal lead (Pb): evidence for a developmental origin and environmental link for AD. J Neurosci. 2008;28:3–9. https://doi.org/10.1523/JNEUROSCI.4405-07.2008.
68. Ximerakis M, Lipnick SL, Innes BT, Simmons SK, Adiconis X, Dionne D, Mayweather BA, Nguyen L, Niziolek Z, Ozek C, Butty VL, Isserlin R, Buchanan SM, Levine SS, Regev A, Bader GD, Levin JZ, Rubin LL. Single-cell transcriptomic profiling of the aging mouse brain. Nat Neurosci. 2019;22:1696–708. https://doi.org/10.1038/s41593-019-0491-3.
69. Xu G, Green CC, Fromholt SE, Borchelt DR. Reduction of low-density lipoprotein receptor-related protein (LRP1) in hippocampal neurons does not proportionately reduce, or otherwise alter, amyloid deposition in APPswe/PS1dE9 transgenic mice. Alzheimers Res Ther. 2012;4:12. https://doi.org/10.1186/alzrt110.
70. Yamada M, Naiki H. Cerebral amyloid angiopathy. In: Progress in molecular biology and translational science, vol. 107. New York: Elsevier; 2012. p. 41–78.
71. Yoon C, Van Niekerk EA, Henry K, Ishikawa T, Orita S, Tuszynski MH, Campana WM. Low-density lipoprotein receptor-related protein 1 (LRP1)-dependent cell signaling promotes axonal regeneration. J Biol Chem. 2013;288:26557–68. https://doi.org/10.1074/jbc.M113.478552.
72. Zhang M, Pan X, Jung W, Halpern A, Eichhorn SW, Lei Z, Cohen L, Smith KA, Tasic B, Yao Z, Zeng H, Zhuang X. A molecularly defined and spatially resolved cell atlas of the whole mouse brain. bioRxiv. 2023. https://doi.org/10.1101/2023.03.06.531348.
73. Zhang Y-L, Wang J, Zhang Z-N, Su Q, Guo J-H. The relationship between amyloid-beta and brain capillary endothelial cells in Alzheimer's disease. Neural Regen Res. 2022;17:2355. https://doi.org/10.4103/1673-5374.335829.
74. Zheng W, Aschner M, Ghersi-Egea J-F. Brain barrier systems: a new frontier in metal neurotoxicological research. Toxicol Appl Pharmacol. 2003;192:1–11. https://doi.org/10.1016/S0041-008X(03)00251-5.
75. Zheng W, Shen H, Blaner WS, Zhao Q, Ren X, Graziano JH. Chronic lead exposure alters transthyretin concentration in rat cerebrospinal fluid: the role of the choroid plexus. Toxicol Appl Pharmacol. 1996;139:445–50. https://doi.org/10.1006/taap.1996.0186.

Publisher's Note